JGR Biogeosciences

RESEARCH ARTICLE
10.1029/2025JG008877

Inclusion of Explicit Soil Freeze-Thaw Dynamics in an Arctic Ecosystem Model Constrains Winter Warming Driven Carbon Loss

Kathleen Savage[1], Susan M. Natali[1], Christina Minions[1], Edward Rastetter[2], Edward A. G. Schuur[3], Jennifer D. Watts[1], and Seeta Sistla[4]

[1]Woodwell Climate Research Center, Falmouth, MA, USA, [2]The Ecosystems Center, Marine Biological Laboratory, Woods Hole, MA, USA, [3]Center for Ecosystem Science and Society, Department of Biological Sciences, Northern Arizona University, Flagstaff, AZ, USA, [4]California Polytechnical Institute, Natural Resources Management & Environmental Sciences, College of Agriculture, Food & Environmental Sciences, San Luis Obispo, CA, USA

Key Points:

- Representation of abiotic drivers in ecosystem models impacts decadal projections of nutrient dynamics in highly seasonal northern biomes
- Climate warming in the cold season and freeze-thaw periods have cascading effects on annual ecosystem carbon and nitrogen allocation
- Temperature-dependent diffusion limitations constrain carbon and nitrogen loss under warming relative to traditional models

Supporting Information:

Supporting Information may be found in the online version of this article.

Correspondence to:

K. Savage,
savage@woodwellclimate.org

Citation:

Savage, K., Natali, S. M., Minions, C., Rastetter, E., Schuur, E. A. G., Watts, J. D., & Sistla, S. (2026). Inclusion of explicit soil freeze-thaw dynamics in an Arctic ecosystem model constrains winter warming driven carbon loss. *Journal of Geophysical Research: Biogeosciences*, *131*, e2025JG008877. https://doi.org/10.1029/2025JG008877

Received 26 FEB 2025
Accepted 6 JAN 2026

Author Contributions:

Conceptualization: Susan M. Natali, Seeta Sistla
Data curation: Kathleen Savage, Christina Minions
Formal analysis: Kathleen Savage
Funding acquisition: Susan M. Natali, Seeta Sistla
Methodology: Kathleen Savage
Visualization: Kathleen Savage
Writing – original draft: Kathleen Savage

Abstract Arctic permafrost soils store vast amounts of carbon (C)-rich organic matter that has accumulated due to low temperatures that suppress microbial decomposition. As Arctic warming intensifies, soil microbes become increasingly active, even while plant growth remains dormant. Seasonal decoupling between plant and microbial decomposer growth can accelerate carbon dioxide (CO_2) release from soils, however, most Earth system models underestimate cold-season C emissions and do not accurately represent the freeze–thaw transitions that govern microbial access to substrates during these critical periods. These model–data mismatches often stem from empirical formulations, such as using a fixed Q_{10} functions to represent microbial respiration, an oversimplification of a complex interplay of temperature, moisture, and substrate diffusion. To address this, we incorporated explicit, temperature-dependent diffusional constraints on microbial activity, (the Dual Arrhenius Michaelis–Menten (DAMM) model), into the Stoichiometrically Coupled Acclimating Microbe–Plant–Soil (SCAMPS) model which uses the Q_{10} function to represent microbial respiration. We used this enhanced model (SCAMPS_DAMM) to simulate Arctic ecosystem responses to a 50-year winter warming scenario and compared outcomes to the original SCAMPS framework. While both models predicted overall soil C losses under warming, SCAMPS_DAMM produced more constrained increases in microbial respiration and plant productivity. These differences led to similar total ecosystem C declines but divergent patterns of C and N allocation between plant and soil pools. Thus, incorporating mechanistic constraints on microbial access to substrates through explicit representation of temperature and moisture controls altered model projections of Arctic biogeochemical responses to climate change.

Plain Language Summary Arctic permafrost soils contain large stores of carbon-rich organic matter. These carbon reserves remain largely unavailable to soil microbes when they are frozen. However, as the Arctic warms, this carbon becomes susceptible to microbially mediated decomposition, which can increase greenhouse gas emissions and further exacerbate climate warming. Ecosystems are dynamically coupled with plant, soil, and microbial decomposer interactions jointly regulating carbon and nitrogen cycling. Models that integrate arctic plant-soil-microbial dynamics improve projections of how thawing permafrost soils will affect the relative balance between carbon storage and release to the atmosphere. We used a biologically coupled plant-soil-microbe model to assess how environmental drivers, such as temperature and moisture, influence predictions of future carbon and nitrogen cycling in Arctic permafrost regions. We found that incorporating a dynamic representation of these environmental factors led to more conservative predictions of carbon loss and shifts in plant productivity under a winter warming climate change scenario. These findings highlight the importance of recognizing how abiotic conditions (e.g., soil moisture availability as frozen soils thaw) are incorporated into mechanistic models and affect projections of how permafrost-dominated ecosystems will respond to ongoing climate warming.

1. Introduction

The Arctic tundra is experiencing more rapid and extreme climate warming than any other biome globally (IPCC, 2019; Rantanen et al., 2022). Arctic permafrost soils contain large stores of carbon (C)-rich organic matter (~1,300 Pg C; Hugelius et al., 2014; Tarnocai et al., 2009), which have accumulated over time due to low temperatures (<0°C) that suppress decomposition (Mikan et al., 2002; Natali et al., 2019; Schuur et al., 2009).

Writing – review & editing: Kathleen Savage, Susan M. Natali, Christina Minions, Edward Rastetter, Edward A. G. Schuur, Jennifer D. Watts, Seeta Sistla

Climate warming stimulates organic matter decomposition, making historically stable C and nitrogen (N) pools biologically available to microbes and plants (Klarenberg et al., 2022), increasing nutrient mineralization and the release of C and N to the atmosphere (Webb et al., 2016).

Arctic climate warming is most extreme during the cold season (Bruhwiler et al., 2021; Watts et al., 2024), when microbial activity is decoupled from plant growth (Huang et al., 2017; Koenigk et al., 2013; Natali et al., 2019). Cold-season C emissions are a major component of the annual tundra C budget (Z. Liu et al., 2024; Natali et al., 2019; Sommerfeld et al., 1993), with decomposition and net ecosystem C exchange highly sensitive to temperature during this period (Arndt et al., 2023; Natali et al., 2014, 2019; Pedron et al., 2022; Sistla et al., 2014). However, most Earth system models have yet to incorporate detailed representations of cold-season C emissions and transitions between frozen and thawed soil states, as highlighted by recent model–data comparisons and model development efforts (He et al., 2014; Hugelius et al., 2024; Tao et al., 2021). These gaps reflect uncertainties in: (a) the controls on cold-season soil C emissions (Grogan, 2012; Wang et al., 2011), especially during the zero-curtain period (when latent heat maintains soil temperatures near 0°C) (Arndt et al., 2019; Outcalt et al., 1990), and (b) how microbial activity during these periods affects plant productivity in the growing season (Natali et al., 2012; Sinsabaugh et al., 2002).

Above- and belowground responses to warming vary across seasonal, annual, and decadal timescales, adding complexity to projections of biogeochemical feedbacks to rapid climate warming (Sistla et al., 2014). Plant–microbe–soil interactions drive competition for available nutrients. Warming can alter microbial community composition and increase plant nutrient uptake, promoting primary production and vegetation shifts toward woody shrubs, while also stimulating soil respiration and microbial nitrogen demand (Y. Liu et al., 2022; Myers-Smith et al., 2020; Poppeliers et al., 2022). A warming-driven shift toward a greener, shrubbier tundra system can in turn affect the quality and quantity of soil organic matter (SOM) inputs, further accelerating (or constraining) microbial decomposer activity (Bracho et al., 2016; Sistla et al., 2013).

Incorporating biologically dynamic, coupled plant–soil–microbe interactions into models can improve ecosystem response projections under warming (Sistla et al., 2014; Trivedi et al., 2022). However, ecosystem models often rely on empirical, rather than mechanistic, representations of biogeochemical processes. For example, microbial decomposition is typically modeled using a Q_{10} function (Davidson et al., 2006; Kirschbaum, 1995), which does not capture the full suite of physical and biophysical constraints, particularly under varying moisture conditions (Bond-Lamberty & Thomson, 2010; Tilston et al., 2010).

This simplification is especially limiting in Arctic soils, which experience prolonged freezing and frequent freeze–thaw cycles. At sub-zero temperatures, Q_{10} values can range from 60 to 200 (Bracho et al., 2016; Mikan et al., 2002), reflecting physical constraints (e.g., reduced liquid water and oxygen diffusion), rather than direct temperature effects (Tilston et al., 2010). As soils freeze, liquid water becomes confined to microsites and air-filled pore space declines, further limiting diffusion (Talamucci, 2003). The static Q_{10} framework fails to capture these nonlinear dynamics (Kurylyk & Watanabe, 2013; Romanovsky & Osterkamp, 2000; Schaefer & Jafarov, 2016) and is the most common representation of biological temperature sensitivity in biogeochemical models.

The Dual Arrhenius Michaelis–Menten (DAMM) model incorporates Arrhenius-based temperature sensitivity and Michaelis–Menten kinetics to explicitly simulate substrate and oxygen limitations (Davidson et al., 2012). Models that explicitly represent substrate and oxygen diffusion limitations offer a more mechanistic alternative to project decomposer response to rapid temperature change during zero-curtain periods. This formulation presents a framework for microbial respiration to respond directly to changes in temperature and liquid water content that can be incorporated into biogeochemical models of warming permafrost systems.

To explore the role of explicit substrate and oxygen diffusion limitations on projected arctic C dynamics with ongoing warming, we integrated DAMM into the Stoichiometrically Coupled Acclimating Microbe–Plant–Soil (SCAMPS) model. SCAMPS couples biologically dynamic, stoichiometrically flexible feedbacks between above and belowground biomass and soil in a permafrost ecosystem (Pold et al., 2022; Sistla et al., 2014). The seasonality of warming and the ability of the microbial community to acclimate (represented by shifts in community-level carbon nitrogen ratio C/N) strongly regulate ecosystem C dynamics in SCAMPS; however, temperature sensitivity in SCAMPS is represented by static Q_{10} submodel for frozen and unfrozen system states. Replacing the Q_{10} approach in SCAMPS with an explicit representation of abiotic drivers (Table 1) that includes a freeze-thaw

Table 1
Model Definitions, Drivers, and Differences Between Model Forms

	Dynamically coupled feedback models		
Model framework name	DAMM	SCAMPS	SCAMPS_DAMM
Abiotic drivers	T, Θ	T	T, Θ
Biotic states	MC, DOC	MC	MC, DOC
Abiotic control on substrate availability		Implicit	Explicit

Note. T—temperature, Θ—liquid water fraction, MC—microbial carbon, DOC—dissolved organic carbon.

sub-model (DAMM) should improve representation of permafrost C cycling under warming climate conditions (Zhou et al., 2024).

We aimed to determine how explicit versus implicit representations of abiotic (soil temperature and liquid water content) constraints on microbial substrate availability influence C and N cycling in an arctic tundra ecosystem with winter warming. We compared the SCAMPS model (with a Q_{10} submodel) to SCAMPS_DAMM, which incorporates explicit abiotic constraints and freeze-thaw dynamics (DAMM submodel) (Table 1). Rather than producing predictive outcomes, this study compares the responses of these two model frameworks under consistent climate forcing to assess how mechanistic constraints alter biogeochemical dynamics. Based on this comparative approach, we hypothesized that:

1. Explicit representation of temperature-dependent diffusion limitations will reduce predicted soil C losses and dampen shifts in C and N allocation under winter warming.
2. These effects will be greatest during the fall zero-curtain period, when soils are thawed and microbial activity is high, but plants are senesced and unable to access released nutrients.

2. Methods

2.1. Model Descriptions

2.1.1. Stoichiometrically Couple Acclimating Microbe-Plant-Soil (SCAMPS) Model

The SCAMPS model couples biologically dynamic feedbacks between above and belowground active soil layer C and N cycling in a permafrost ecosystem (Figure 1, Table 2); a full description of the model can be found in Sistla et al. (2014). SCAMPS is a daily time-step, soil temperature-driven mechanistic model of arctic tundra systems that represents the potential plasticity of the soil microbial and plant communities to stressors such as warming and natural variation such as seasonal temperature shifts (Pold et al., 2022; Sistla et al., 2014). This biological plasticity is represented through shifts in the optimal microbial and plant community C/N that reflects changes in the stoichiometry of available substrates, with resource allocation tightly coupled to organismal and ecosystem stoichiometry using a resource allocation optimization model (Rastetter et al., 1997, 2013). For microbes, changes in C/N are inferred representations of functional adaptation rather than explicit simulations of microbial functional group composition or diversity (Buckeridge et al., 2013).

Plant productivity is mechanistically coupled with soil N availability through stoichiometric constraints, where plant growth is limited by the uptake of inorganic N from the soil, and this N availability is dynamically regulated by microbial decomposition, mineralization, and competition for nutrients based on microbial C:N demands, decomposer biomass, soil temperature and substrate availability (quantity and quality (Pold et al., 2022; Sistla et al., 2014)).

A major advancement of the SCAMPS model is the dynamic representation of microbially synthesized extracellular enzymes, which catalyze the breakdown of polymeric detritus that is then assimilated by decomposers (Sinsabaugh et al., 2008). Extracellular enzymes link plant inputs and soil conditions to the decomposer community and soil C and N cycling. SCAMPS represents microbial extracellular enzyme activities as an integrated response to highly dynamic soil temperature changes and longer-term interactions between plant-derived soil inputs, the decomposer community, and edaphic factors. SCAMPS represents dynamic feedbacks among plants, microbes, and soil biogeochemical processes: microbial biomass can shift toward a more fungal (higher C/N) or bacterial (lower C/N) community in response to changes in the soil environment while the plant community can

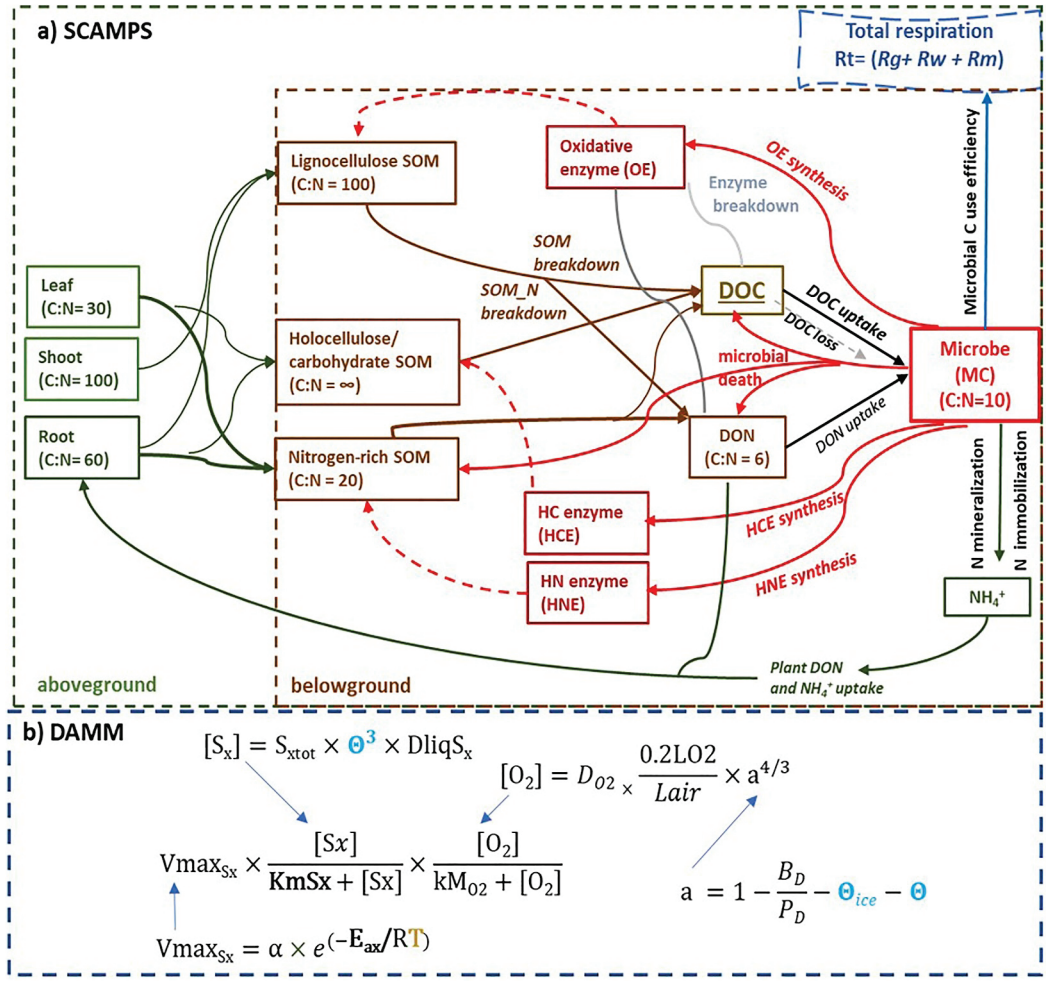

Figure 1. Conceptual diagram of the (a) SCAMPS. Boxes are carbon pools (g C m^{-2}), solid arrows represent flow between pools, and dashed arrows represent processes. Total heterotrophic (microbial) respiration (Rt) is the sum of maintenance (Rm), growth (Rg) and waste (Rw) respiration. See Table 2 for parameter details. MC—microbial carbon, MN—microbial nitrogen, qmicB is the optimal C/N. (b) DAMM model. **Bold** are fitted parameters based on field observations. T—soil temperature, and θ is liquid water fraction and is integrated to control substrate Sx and O_2 diffusion. θ_{ice} is frozen water fraction. See Sistla et al. (2014) for full SCAMPS model description including pools and fluxes; and Davidson et al. (2012) for full DAMM model descriptions. See Supporting Information S1 SCAMPS model code.zip for a complete description of SCAMPS and the fitted DAMM model parameters.

shift between a more graminoid and woody-dominated system depending on soil temperature and nutrient availability. Therefore, warming-driven changes in the biological components of the model dynamically shift its nutrient balance and fluxes.

SOM in SCAMPS is separated into three pools of varying chemical recalcitrance and C/N that is representative of tussock tundra active layer soils. Microbial biomass (MB) synthesizes distinct enzymes for each SOM pool (Figure 1a) that varies based on the microbial C/N and substrate availability, which break down SOM pools releasing C and N into the system. Available C and N, in the form of dissolved organic carbon (DOC) and dissolved organic nitrogen (DON) are a balanced sum from each of these SOM pools. Nitrogen is conserved within the system; however, C can be lost via leaching of DOC, and C, in the form of CO_2, is lost from microbial carbon (MC) through respiration, represented as total heterotrophic (microbial) respiration (Rt) and is the sum of maintenance respiration (Rm), growth respiration (Rg) and waste respiration (Rw) (Figure 1a). Autotrophic respiration is not represented in the SCAMPS model. The SCAMPS model simulates the dynamic feedback between above and belowground communities using temperature as its seasonal driver, with substrate quantity and quality further regulating decomposition potential. Rm and Rw are temperature sensitive, with a different Q_{10}

Table 2
Definition of Drivers and Parameters in the SCAMPS, Q_{10}, and DAMM Models, Shown in Figure 1

Microbial respiration	R_m	Maintenance respiration (g C m^{-2})
	R_w	Waste respiration (g C m^{-2})
	R_g	Growth respiration (g C m^{-2})
	R_t	Total respiration (Rm + Rw + Rg) (g C m^{-2})
Abiotic drivers	T	Soil temperature (°K)
	Θ	Liquid water fraction
	$Θ_{ice}$	Frozen water fraction
C pool	MC	Microbial carbon (g C m^{-2})
	DOC	Dissolved organic carbon (g C m^{-2})
DAMM Substrate	S_x	Substrate available (g C m^{-2})
	O_2	Oxygen concentration (modeled)
Constants	a	Air filled porosity (%)
	B_D	Bulk density (g cm^{-3})
	P_D	Particle density (g cm^{-3})
	R	Universal gas constant (kJK^{-1} mol^{-1})
DAMM fitted parameters	α	Preexponential constant (g C m^{-2})
	E_{ax}	Activation energy (kJmol^{-1})
	K_m	Half saturation constant (g C m^{-2})

Note. For a full accounting of SCAMPS_DAMM model parameter in Figure 1 see parameter file in the attached SCAMPS model code.zip file.

function dependent on whether soil temperature is above ($Q_{10} = 6$) or below freezing ($Q_{10} = 60$). The differing Q_{10} function for microbial processes implicitly incorporates substrate limitation via diffusion as the soil temperature transitions across the freezing threshold. The high Q_{10} value below freezing is representative of the microbial respiration response to a combined temperature and ice-liquid moisture dynamics and derived from arctic tundra soil incubation studies.

2.1.2. Dual Arrhenius Michaelis-Menten Model (DAMM)

DAMM is a parsimonious process-based model that represents soil heterotrophic (Rt) respiration is regulated by changing temperature, substrate supply Sx,-dissolved organic carbon (DOC); and O_2, and moisture (Figure 1b). DAMM simulates soil enzymatic process using Michael-Menten, Arrhenius, and diffusion equations using temperature and Sx to regulate heterotrophic respiration. Temperature-dependent diffusion equations simulate the supply of substrates to reactions sites, controlled by air filled pore space (porosity, a). Sx diffusion is limited by the presence of liquid water (Θ) and ice via changes in air-filled pore space.

2.1.3. Freeze-Thaw Model

Microbial respiration has historically been assumed to be zero within frozen soils; however, recent in situ measurements and incubations have shown that microbial respiration occurs below freezing temperatures, to as low as −20°C (Bracho et al., 2016; Mikan et al., 2002). This activity is supported by a thin film of liquid water surrounding soil particles even when the soil drops below freezing, allowing microbes to access substrate at the microsite level (Panikov & Sizova, 2007; Schaefer & Jafarov, 2016; Sihi et al., 2020). A freeze-thaw model to estimate liquid (Equation 1a) and frozen water (Equation 1b) below 0°C based on temperature and soil texture (sand, silt, clay and organic content) is incorporated within the DAMM model (Figure 1b).

$$\theta = \left(\frac{T_{\text{ref}} - T}{T*}\right)^{b} \tag{1a}$$

$$\theta_{\text{ice}} = \theta_{\text{crit}} - \theta \tag{1b}$$

where: Equation 1a Θ—soil liquid water fraction (unitless), Tref-reference temperature (°C), b-an empirical constant defined by soil texture, T^*-temperature offset (°C), T-observed soil temperature, and Equation 1b Θ_{ice}—fraction ice, Θ_{crit}—maximum liquid water fraction at 0°C (Schaefer & Jafarov, 2016—see Table 1 in Schaefer & Jafarov, 2016) and Θ—liquid water fraction.

2.1.4. SCAMPS_DAMM

Maintenance respiration, Rm, is represented by a Q_{10} function in SCAMPS, with differing Q_{10} values above and below 0°C (Figure 1b). In SCAMPS_DAMM, this representation of Rm was replaced with the DAMM function, including a freeze-thaw component to explicitly represent biological and physical drivers (Figure 1b) at above and below freezing. SCAMPS_DAMM thus adds temperature-dependent diffusion limitation on substrate supply (DOC and O_2) not explicitly represented within SCAMPS (Figure 1b, Table 2).

Microbial waste respiration (Rw) in SCAMPS occurs only when the microbial C/N ratio exceeds the optimal C/N ratio. When this occurs the microbial modifier (MC/MN * optimal C/N) is multiplied by the Q_{10} function to estimate loss of carbon via microbial waste. In SCAMPS_DAMM, the Q_{10} function is replaced by the DAMM equation (Figure 1b), leaving the C/N ratio modifier. Growth respiration (Rg) is not directly temperature-dependent in SCAMPS but occurs when microbial uptake exceeds C loss from Rm.

2.2. Site Description

DAMM model parameters were derived from observations of C flux, temperature, moisture, and soil properties from Eight Mile Lake, Alaska (ELM; 63° 59′N, 149° 15′W) Alaska (EML; Mauritz et al., 2016; Minions et al., 2020; Schuur et al., 2007) (Table 2, Figure 1b). SCAMPS was originally parameterized based on environmental conditions at Toolik Field Station, Alaska (68° 38′N, 149° 36′W). Both Toolik and Eight Mile Lake are moist acidic tussock tundra with similar vegetation composition and belowground carbon. However, Toolik is a colder, higher latitude system (Table S1 in Supporting Information S1). For this modeling framework comparison, we used soil respiration (Rs) data collected at EML to parameterize DAMM prior to incorporation into SCAMPS. For model framework comparison and the winter warming scenario, we used the original SCAMPS environmental parameters available in Sistla et al. (2014) and in the supplementary modeling code.

2.3. Observed Soil Respiration Data

Observed soil respiration (Rs = belowground autotrophic, Ra, + microbial, Rt, respiration) was measured at Eight Mile Lake from 2018 to 2021 using forced diffusion sensors (FD; Minions et al., 2020). These data, along with soil temperature (HOBO S-TMB-M006 Temperature Smart Sensor) and moisture (HOBO S-SMD-M005 10HS Soil Moisture Smart Sensor), were used to constrain the parameterization of the DAMM and Q_{10} submodel.

Outliers in Rs, primarily occurring during freeze-thaw transitions, were removed from the analysis (Figure S1 in Supporting Information S1). Values near 0°C may reflect rapid degassing of accumulated CO_2 during thaw, rather than the microbial response under ambient conditions (Stackhouse et al., 2015). In some cases, measured or modeled SR rates just below 0°C exceeded peak summer fluxes, indicating abiotic contributions. To account for this, the mean SR flux between −1 and 1°C was used as an estimate of maximum below-freezing respiration rate. Across the 2018–2021 period, 682 daily Rs measurements were collected; after outlier removal, 491 measurements (72%) remained for analysis.

2.3.1. Rs Adjustments to Account for Belowground Autotrophic (R_a) and Heterotrophic-Microbial (R_t) Respiration

Observed total soil respiration (Rs) at Eight Mile Lake includes both autotrophic (Ra) and heterotrophic (Rt) components, whereas the Q_{10}, DAMM, SCAMPS, and SCAMPS_DAMM models simulate only Rt. To compare observations with model output, Rs was adjusted for the seasonal contribution of Ra (Hicks Pries et al., 2016): winter 0%, shoulder seasons 15%–25%, and summer up to 45%, yielding an estimate of heterotrophic respiration, Rt_obs.

In SCAMPS, Rt comprises maintenance (Rm), waste (Rw), and growth (Rg) respiration:

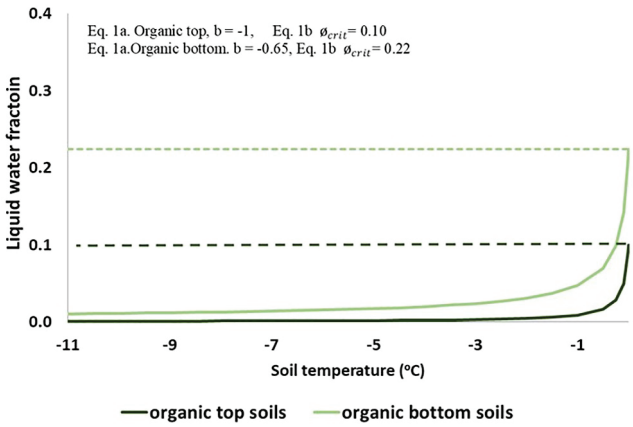

Figure 2. Estimated liquid water (moisture) fraction for EML at below freezing temperatures. From Schaefer and Jafarov (2016). Soil profiles are organic soils with greater bulk density at depth. Organic top 0–15 cm, organic bottom 15–25 cm. ϕ_{crit} for soils shown as dashed lines for each soil horizon.

$$\mathrm{Rm} = \mathrm{resp}_{\mathrm{mic}} \cdot \mathrm{MC} \cdot Q_{10}^{\frac{T}{10}} \quad (2a)$$

$$\mathrm{Rw} = \mathrm{resp}_{\mathrm{waste}} \cdot \left(\mathrm{MC} - q_{micB} \cdot \mathrm{MN}\right) \cdot Q_{10}^{\frac{T}{10}} \quad (2b)$$

$$\mathrm{Rg} = \frac{\mathrm{resp}_{\mathrm{growth}} \cdot \mathrm{Gr}_{\mathrm{mic}}}{1 + \mathrm{growthresp}_{\mathrm{rate}}} \quad (2c)$$

Because Rm and Rw vary with temperature, while Rg is not directly temperature-sensitive, we excluded Rg from Rt_obs during Q_{10} and DAMM submodel calibration (Section 2.4). The exclusion was based on the proportion of daily Rg to Rt estimated from a previous SCAMPS simulation under ambient temperature conditions (Sistla et al., 2014), minimizing potential overestimation of temperature effects.

2.3.2. Freeze-Thaw Model

Freeze-up occurs from both the permafrost below and the soil surface above, allowing liquid water to persist at depth even when surface soils are frozen. Microbial activity was assumed to peak where soil temperatures were highest, near the surface in summer and deeper in winter (Figure S2 in Supporting Information S1). Liquid water content was estimated using organic soil characteristics above 25 cm depth, and denser organic estimates below (Figure 2). The freeze-thaw model dynamically incorporates changes in air filled pore space; however, the model does not depict ice lenses, which can fully restrict diffusion into and out of the soil profile.

2.3.3. SCAMPS Model Modifications

Eight Mile Lake Rt_{obs} fluxes, soil temperature, liquid water content between 2018 and 2021 (Figures S3a and S3b in Supporting Information S1), and daily DOC (Figure S3c in Supporting Information S1, from Sistla et al., 2014) were used to derive DAMM parameters α, E_a and K_m (Table 1, Figure 1b). When soil was below 0°C, its relative liquid water and ice contents were determined from Equations 1a and 1b (Figure 2). When soil was above 0°C, soil moisture was based on observations from Eight Mile Lake (Figure S3b in Supporting Information S1). Porosity varies by depth relative to liquid water and ice fraction, and bulk density (B_D). At <25 cm deep, B_D was set to 0.10 and 0.40 g cm^{-3} at greater than 25 cm depth (Bracho et al., 2016); these differences in B_D are reflected in the change in prediction of liquid water and ice, with deeper depths having denser organic layer compared to shallower organic layer depths.

SCAMPS was originally parameterized for a higher latitude tussock tundra ecosystem (i.e., Toolik Lake, AK) than Eight Mile Lake (Sistla et al., 2014); its original Q_{10} function parameters overpredicted Rt compared to observations (Rt_{obs}) when using warmer soil temperatures characteristic of Eight Mile Lake. To account for this difference, the Q_{10} function in SCAMPS was reduced from 6 to 5 at temperatures >0°C but remained at 60 when the soil temperature was below 0°C. To ensure modeled C pools in SCAMPS_DAMM were comparable to the original versions (Sistla et al., 2014), small modifications were made to additional parameters (Table S2 in Supporting Information S1). The DAMM model parameters were fit using least squares regression. The Arrhenius activation energy (Ea) in DAMM can be representative of an array of substrate reactions, however in this model comparison we do not include varying activation energies.

2.4. Q_{10} and DAMM Sub Model Parameterization and Validation

To assess Q_{10} and DAMM model fit we used a linear regression between predicted versus observed Rm (R^2 and RMSE). The parameters from these model fits (Q_{10} for SCAMPS; Eax, α, and Km for SCAMPS_DAMM) were incorporated into each model framework.

The DAMM model improved overall fit (R^2 = 0.51, RMSE = 0.29) compared to the Q_{10} model (R^2 = 0.49, RMSE = 0.30) with DAMM better at capturing Rt_{obs} at freeze-thaw temperatures near 0°C, while the Q_{10} function predicted higher rates of respiration at warmer temperatures (Figure 3). Figure S3a in Supporting

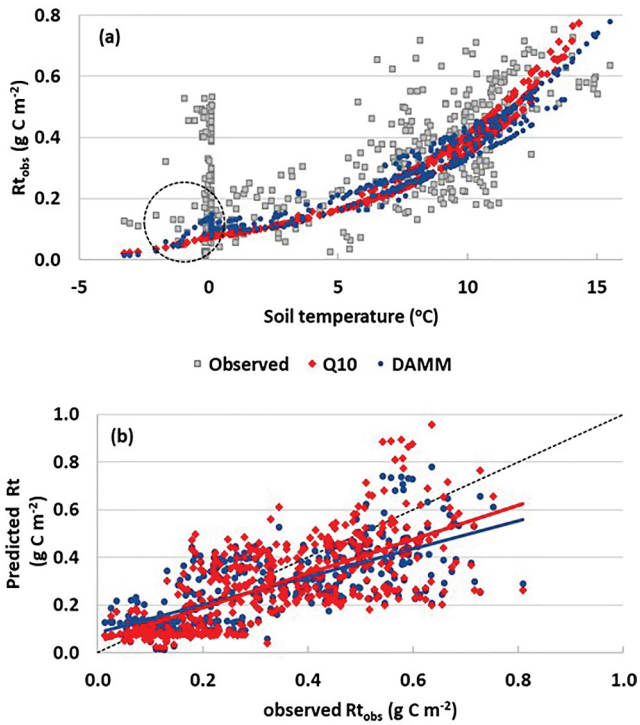

Figure 3. Modeled and observed soil fluxes from EML. (a) Predicted Rt and observed Rt_{obs} using Q_{10} and DAMM model fits, plotted against soil temperature. Dashed circle shows the effects of the freeze-thaw model. (b) Model fits to observed values. (a) Circle denotes capture of freeze-thaw transition. (b) Dashed line is 1:1.

Information S1 shows the observed and predicted respiration versus time for the Q_{10} and DAMM models for the 2018–2021 period at Eight Mile Lake.

2.5. Climate Warming Simulation

The SCAMPS and SCAMPS_DAMM models were spun up to equilibrium (500 years) to compare how each model configuration would allocate C and N pools under implicit (SCAMPS) versus explicit (SCAMPS_DAMM) representations of moisture and substrate availability. We compared ecosystem responses to ambient soil temperature with a 50-year soil winter warming scenario (described in Pold et al., 2022) to test the impact of including a temperature-dependent diffusion limitation with the SCAMPS_DAMM model (Figure 1b). The winter period was defined as day of year (DOY) 1–115, summer as DOY 116–248 and fall as DOY 249 to 365. The warmed scenario increased soil temperatures by 0.048°C yr^{-1}, during the winter and fall season (DOY 248 to 116) consistent with the 50-year increase in mean annual air temperatures predicted by CMIP5 downscaled to Anaktuvuk Pass, AK, USA under a moderate (RCP 6.5) emissions scenario (Van Vuuren et al., 2011; Walsh et al., 2018). During the shoulder season, soil temperature increased by 4.9°C over ambient conditions in 0.98°C increments from September (day of year 249–273) and returned to the baseline conditions in late April, (day of year 91–115, Figure 4a). This scenario reflects that winter and shoulder season (winter to spring and summer to fall transition) temperatures are predicted to warm disproportionately in tundra systems with the fall seeing the largest increase in temperature (Arndt et al., 2019; Sturm et al., 2005).

After 50 years of simulated warming, the model was run at the final elevated soil temperature for an additional 50 years (YR51- YR100) to explore the ecosystem response to a new steady state soil temperature and moisture relative to continued ambient conditions (Figure S4 in Supporting Information S1).

2.6. SCAMPS and SCAMPS_DAMM Model Implementation

The R package ("R Core Team," 2021) desolver (Soetaert et al., 2010) was used for resolving the differential equations in SCAMPS and SCAMPS_DAMM, using the variable step method of the fourth and fifth orders Runge-Kutta. The overall objective of this work is to assess the impact of including a temperature dependent diffusion constraint (SCAMPS_DAMM) on predictions of carbon and nitrogen allocation under a winter warming scenario. We evaluate this by (a) comparison between SCAMPS and SCAMPS_DAMM model outcomes (b) a parameter sensitivity analysis.

2.7. Parameter Sensitivity Analysis

We conducted a Monte Carlo–based global sensitivity analysis for SCAMPS and SCAMPS_DAMM using randomly generated parameter combinations. The analysis tested temperature sensitivity parameters (Q_{10} for SCAMPS; *Eax*, α and *KmSx*, for SCAMPS_DAMM) and nutrient uptake parameters (plant uptake of DON and NH_4^+; microbial uptake of DOC, DON, and NH_4^+). Parameter values were varied uniformly within ±10% of their baseline estimates, and 50 model iterations were run for each configuration. To compare the model output between SCAMPS and SCAMPS_DAMM we used the same initial carbon and nitrogen pools to remove variation due to differing initial states. This Monte Carlo approach, implemented using the R FME package (Soetaert & Petzoldt, 2010), quantifies the influence of parameter uncertainty on model outputs. Model code to perform the sensitivity analysis and parameter files are provided in Supporting Information S1.

3. Results and Discussion

Plant and microbes are biologically coupled while operating on distinct spatial and temporal scales, dynamically allocating nutrients to above and belowground pools within a shared soil environment. We compared the effects

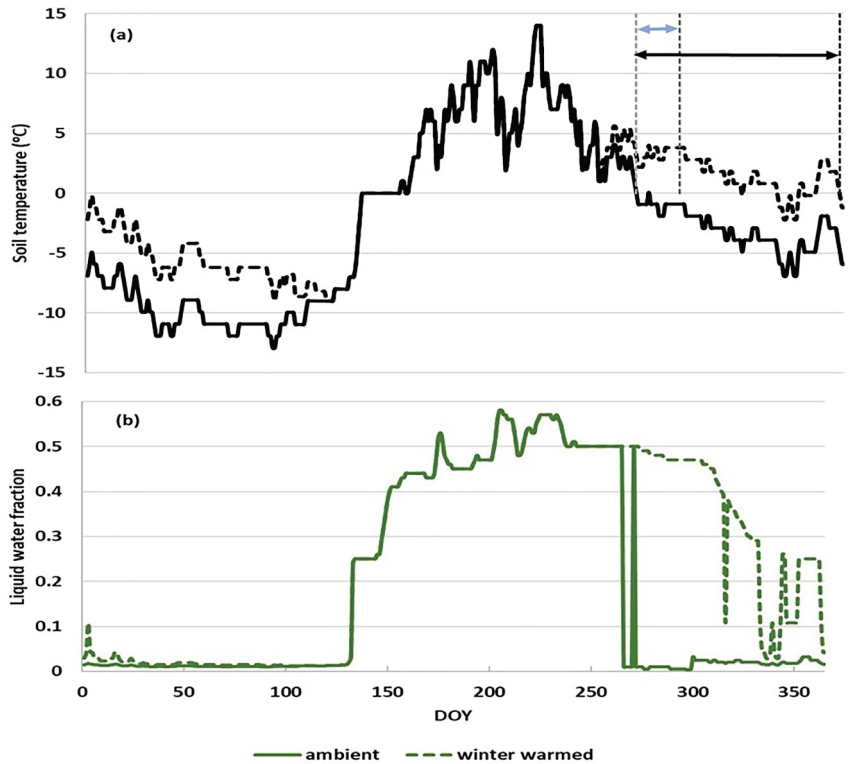

Figure 4. Daily (DOY) abiotic drivers: (a) soil temperature, (b) available liquid water fraction. Solid lines = ambient; dashed = winter warming at YR50. Vertical dashed lines in (a) show the fall zero-curtain period, from original (blue) to extended above-freezing period under warming (black).

of explicit versus implicit modeling of abiotic (temperature, moisture) drivers on substrate diffusion to decomposer microsites and subsequent projections of permafrost ecosystem dynamics under a 50-year gradual winter warming, followed by 50 years at elevated temperatures relative to ambient active layer temperatures. SCAMPS_DAMM had more constrained annual changes in tundra C and N pool sizes and fluxes under ambient soil temperature conditions and dampened increases in microbial respiration and shifts in ecosystem C and N pools relative to SCAMPS under winter warming. These differences highlight the importance of the explicit representation of liquid water and ice content as a constraint on both microbial activity and, indirectly, plant productivity in permafrost ecosystems.

3.1. Ecosystem Carbon and Nitrogen Resource Allocation Under Ambient Climate Conditions

At steady state under ambient conditions, SCAMPS and SCAMPS_DAMM produced distinct C and N pool distributions and fluxes despite having identical soil temperature. SCAMPS simulated smaller microbial and plant C and N pools, larger soil C stocks and lower annual (Rt) respiration (Table 3a). These differences arise from SCAMPS_DAMM's explicit representation of temperature-dependent diffusion, which links soil moisture and ice dynamics to substrate and O_2 availability. Microbial activity in SCAMPS_DAMM is more strongly constrained by diffusional processes than by substrate abundance. This mechanistic coupling moderates Rt and nutrient (C and N) turnover under baseline conditions. The modeled behavior aligns with field observations of microsite-scale heterogeneity and moisture control of respiration in frozen soils (Mikan et al., 2002; Schaefer & Jafarov, 2016; Tilston et al., 2010); however, temperature-dependent diffusional constraints are poorly captured in mechanistic models limiting our predictive ability of permafrost ecosystem biogeochemical responses to climate warming. The distinct steady states of SCAMPS and SCAMPS_DAMM under ambient conditions set different initial C and N distributions, which frames their responses to the winter warming scenario.

Table 3
Annual Average C and N Pools and Fluxes Under Current (Steady State) and Winter-Warming (w.w.) Scenarios at YR 50 and YR 100 (g C or N m^{-2} yr^{-1})

		a) Steady state (ambient)		b) Winter warming YR 50 (non-steady state)		c) Winter warming YR 100 (new steady state)	
		SCAMPS	SCAMPS_DAMM	SCAMPSw.w	SCAMPS_DAMMw.w	SCAMPSw.w	SCAMPS_DAMMw.w
Microbial biomass	MC	78	99	114 (146)	116 (117)	99 (127)	95 (96)
	MN	7.9	10.0	12.6 (159)	13.6 (137)	11.0 (139)	11.1 (111)
	Microbial C/N	9.9	10.0	9.0	8.5	8.9	8.5
Nutrient pools	DOC	5.7	6.3	3.0	3.4	2.8	2.9
	DON	0.5	0.5	0.3	0.3	0.3	0.3
	NH_4^+	0.4	0.4	0.2	0.3	0.2	0.3
Belowground carbon and nitrogen pools	ppSOM	2,392	2,304	2,229 (93)	2,168 (94)	2,206 (92)	2,208 (96)
	hcSOM	1,705	1,600	1,219 (71)	1,059 (66)	1,153 (68)	1,053 (66)
	N-rich SOM	834	763	697 (84)	660 (87)	753 (90)	763 (100)
	Belowground C	**4,931**	**4667**	**4,145 (84)**	**3,887 (83)**	**4,113 (83)**	**4,025 (86)**
	N-rich SOM - N	37	34	31	29	33	34
	ppSOM - N	24	23	22	22	22	22
	Belowground N	**61**	**57**	**53 (87)**	**51 (89)**	**55 (90)**	**56 (98)**
Plant carbon and nitrogen pools	Wood carbon	157	181	202 (129)	220 (121)	196 (125)	187 (97)
	Leaf carbon	74	82	91 (123)	98 (120)	88 (119)	83 (101)
	Root carbon	263	304	338 (128)	368 (121)	330 (125)	314 (103)
	Plant C	**494**	**574**	**630 (127)**	**687 (121)**	**614 (124)**	**584 (102)**
	Wood nitrogen	1.6	1.8	2.0	2.2	2.0	1.9
	Leaf nitrogen	2.6	3.0	3.3	3.6	3.2	3.0
	Root nitrogen	4.4	5.1	5.7	6.2	5.5	5.3
	Plant N	**8.6**	**9.9**	**11.0 (128)**	**12.0 (121)**	**10.7 (124)**	**10.2 (103)**
	Litter biomass	114	130	145	158	141	134
	Ecosystem carbon	**5,617**	**5,463**	**5,034 (90)**	**4,847 (89)**	**4,967 (88)**	**4,838 (89)**
Microbial carbon fluxes	Rt	55.9	61.8	101.8 (182)	99.7 (161)	87.4 (156)	81.7 (132)
Abiotic drivers	Mean soil T	−2.3	−2.3	0.3	0.3	0.3	0.3
	Mean soil Θ	na	0.18	na	0.27	na	0.27

Note. Mean T = annual soil temperature (°C); mean θ = annual liquid water fraction. Values in () show percent change relative to steady state (values <100 = loss, >100 = gain). Pools differ slightly at steady state across models due to dynamic feedbacks. pp = polyphenolic, hc = holocellulose, Rt = total respiration (Rm + Rg + Rw), Ecosystem C = belowground C + plant C + litter + MC, Belowground C = ppSOM + hcSOM + N-rich SOM, Belowground N = N-rich SOM - N + ppSOM - N, Plant C = wood carbon + leaf carbon + root carbon, Plant N = wood nitrogen + Leaf nitrogen + root nitroge.

3.2. Changes in the Fall Zero-Curtain Period Drive Year-Round Shifts in Nutrient Resource Allocation

The relatively stronger microbial activity stimulated by fall shoulder season warming (Figure S5a in Supporting Information S1) also led to greater microbial N demand (Figure S5b in Supporting Information S1) in SCAMPS_DAMM, which intensified plant–microbe competition during the subsequent growing season. This amplified microbial nutrient draw-down constrained early-season plant N uptake and shifted it to later in the season, limiting aboveground growth. Together, these dynamics explain why SCAMPS_DAMM produced more constrained summer plant C accumulation and respiration, despite enhanced winter microbial activity. This feedback mechanism, where winter microbial activity indirectly suppresses summer C fluxes, illustrates the importance of seasonal coupling between microbial and plant nutrient dynamics.

As Arctic regions warm, the fall zero-curtain period, when soil temperatures remain near 0°C, has been extending later into the season (Arndt et al., 2019). This transitional period plays a critical role in carbon (C) and nitrogen (N) cycling by influencing overwinter microbial respiration and the early-season release of nutrients for plant uptake (Figure S5e in Supporting Information S1). Although CO_2 pulses during zero-curtain periods have been

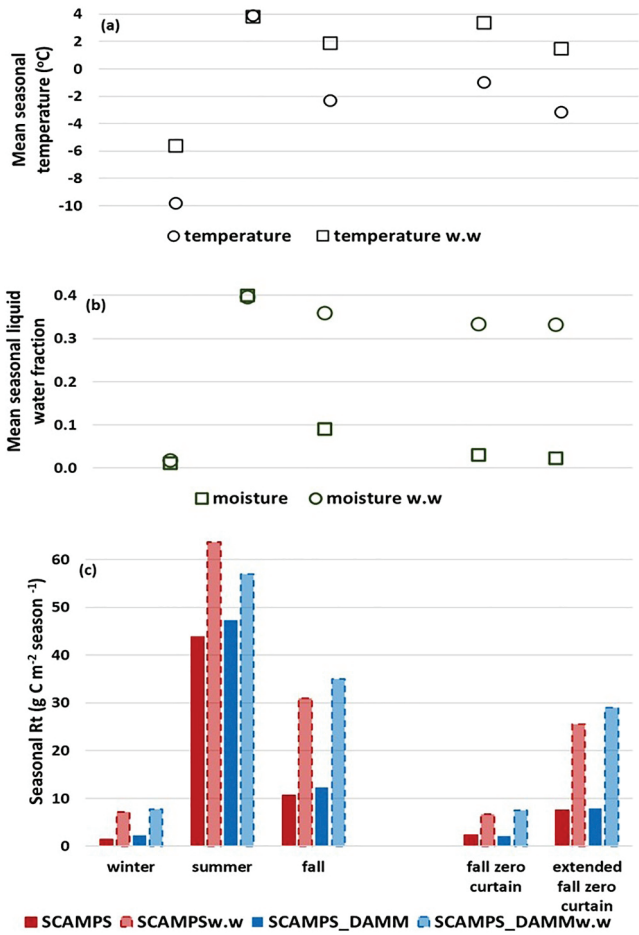

Figure 5. Seasonal dynamics after 50 years under ambient and winter-warming (w.w.) scenarios: (a) mean soil temperature, (b) available liquid water, and (c) total soil respiration (Rt). Seasons: winter (DOY 1–115), summer (DOY 116–248), fall (DOY 249–365). Fall zero-curtain: ambient DOY 265–286; extended w.w. DOY 265–365 (see Figure 4). See Table S3 in Supporting Information S1 for Rt changes and Figure S7 in Supporting Information S1 for monthly temperature, water, and Rtotal patterns.

observed in field studies (Byrne et al., 2022; Commane et al., 2017), they are rarely represented explicitly in ecosystem models.

Under the winter-warming scenario, the fall zero-curtain period lengthened from 21 days under ambient conditions to 98 days after 50 years of warming (Figure 4). This extension led to a marked rise in liquid-water availability, with mean daily soil temperatures near freezing and liquid water content increasing until YR 41, when soils were fully thawed in fall (Table S3 in Supporting Information S1). After YR 41, available liquid-water plateaued even as mean annual temperature rose another 0.25°C (Figure S4 in Supporting Information S1), indicating a threshold where additional warming no longer increases water availability.

These seasonal dynamics directly affect ecosystem fluxes. Under winter warming, SCAMPS_DAMM predicted greater annual C loss (29%) than SCAMPS (25%) after 50 years (Figure 5). The difference reflects how the explicit representation of diffusion in SCAMPS_DAMM links soil temperature and moisture to substrate and oxygen transport, whereas SCAMPS responds implicitly and statically to temperature and moisture via Q_{10} scaling. As liquid-water availability remained high during the extended fall zero-curtain, microbial activity in SCAMPS_DAMM intensified, producing higher respiration and N mineralization (Figure S5e in Supporting Information S1) when plants were dormant overwinter. This decoupled decomposition from plant uptake, creating short-term N surpluses.

Microbial community composition also diverged between models. SCAMPS_DAMM simulated a shift toward more bacterial-like decomposers with lower C:N ratios and higher N demand, increasing microbial competition with plants and reducing productivity gains under warming. These patterns were mirrored in modeled NH_4^+ availability and microbial C:N ratios (Figure S5c in Supporting Information S1), supporting the hypothesis that explicit diffusion constraints most strongly affect ecosystem function during the fall zero-curtain, when microbial processes remain active, but plant uptake is minimal.

From a process-model perspective, these results emphasize that zero-curtain dynamics act as a seasonal "control point" for tundra C and N cycling. Explicitly representing diffusion and freeze-thaw dynamics allows the model to capture transitional shifts in microbial activity and nutrient turnover that drive long-term ecosystem feedbacks under asymmetric winter warming.

3.3. Mechanistic Insights and Model Implications for Decadal Ecosystem Dynamics

We tested whether implicit (Q_{10}-based) versus explicit (diffusion-limited) representations of liquid-water control on decomposition alter projected ecosystem trajectories under a 50-year winter-warming period followed by 50 years of steady state (Table 3, Figure 6). This structural difference produced distinct decadal C–N dynamics even under identical thermal forcing, addressing the hypothesis that explicit representation of temperature-dependent diffusion would reduce soil C losses and dampen shifts in resource allocation under warming.

Winter warming disproportionately affected the fall zero-curtain period, when soils remained near 0°C. During this transition, the fraction of fall days above freezing increased from 37% in YR1 to 58% in YR41, raising mean liquid-water content until soils were fully thawed by YR41 (Figure S4 in Supporting Information S1). Beyond that point, liquid water no longer increased despite continued temperature rise. These dynamics governed differences in microbial respiration and C–N feedbacks between the model frameworks.

Cumulative Rt peaked earlier in SCAMPS_DAMM (YR 41) than in SCAMPS (YR 50) (Figure 6a), reflecting that respiration in the explicit model equilibrated once diffusion no longer limited substrate supply, whereas the implicit Q_{10} formulation continued to respond to temperature. This process coupling produced more dynamic

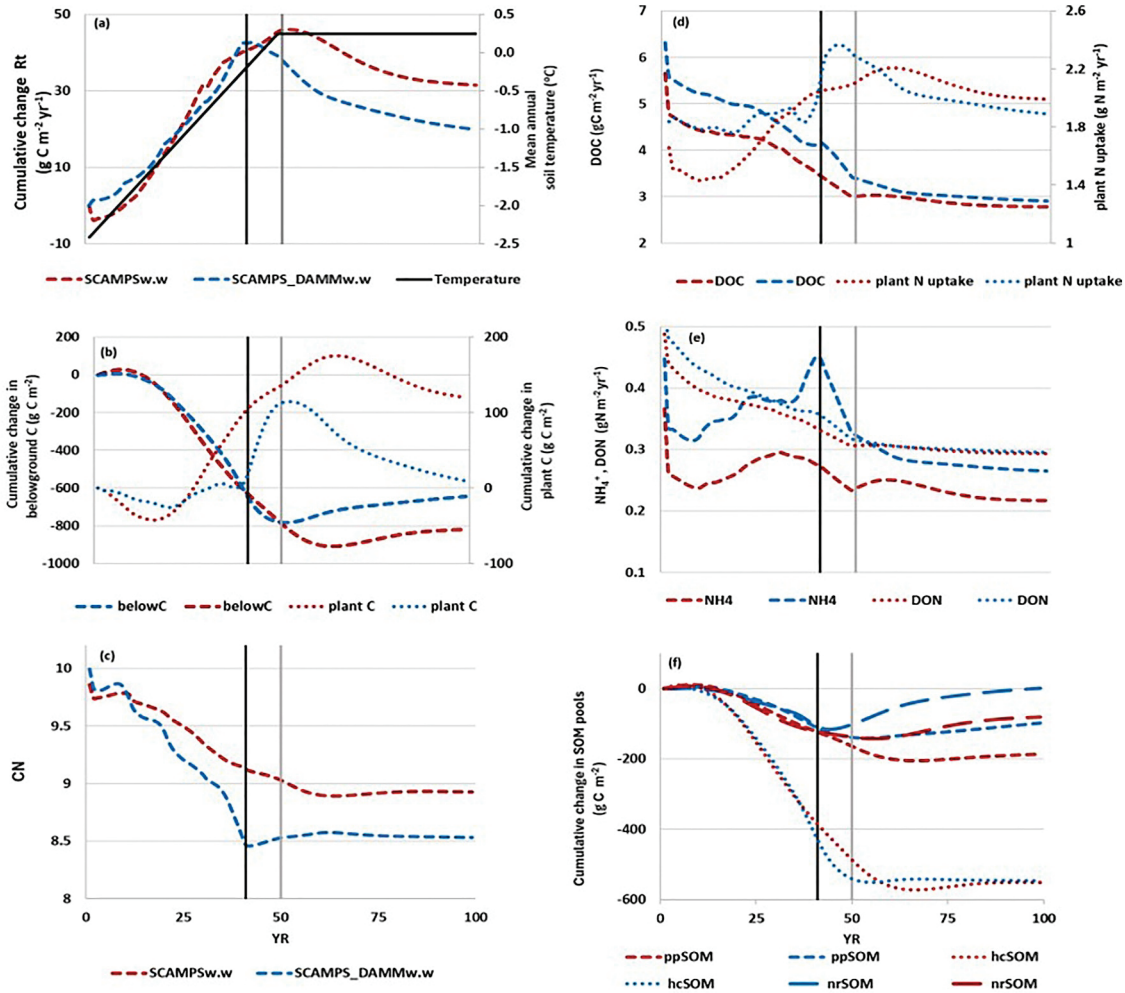

Figure 6. Winter-warming scenario over 100 years, with warming applied for the first 50 years and steady-state temperatures thereafter. Panels show: (a) cumulative change in Rt and mean annual soil temperature, (b) cumulative change in total belowground (SOM) and plant C pools, (c) mean annual C/N ratio, (d) mean available DOC and annual change in plant N uptake, (e) mean annual NH_4^+ and DON, and (f) cumulative change in each SOM pool. Black and gray lines indicate years 41 and 50, respectively. Dark red denotes SCAMPSw.w and blue denote SCAMPS_DAMMw.w (unless otherwise indicated). See Figure S6 in Supporting Information S1 for annual C allocation to wood, leaves, and roots.

shifts in plant biomass, available N, and ecosystem C/N (Figures 6b–6e). The explicit representation of substrate transport allowed SCAMPS_DAMM to respond to both temperature and liquid-water change during freeze–thaw transitions, producing faster microbial and nutrient feedbacks under non-steady-state warming.

The tighter coupling of temperature and diffusion processes in SCAMPS_DAMM also produced indirect effects on plant productivity. Enhanced microbial activity and N mineralization during winter increased microbial N immobilization, reducing early spring N availability for plant uptake. As microbial communities shifted toward more bacterial-like assemblages and preferentially decomposed less N-rich substrates, less mineral N was released to the soil, further constraining plant nutrient supply (Figure 6d). Consequently, NH_4^+ availability and plant uptake shifted later in the season, with uptake occurring under cooler conditions near dormancy, limiting overall plant growth and C accumulation. This feedback loop suppressed summer respiration rates, even though microbial metabolism was more active during the cold season.

After 100 years of warming, both models predicted SOC loss, but their trajectories differed. SCAMPS_DAMM showed minimal reduction in recalcitrant (ppSOM) and N-rich (nrSOM) pools, yet greater depletion of labile hcSOM (Table 3). Increased targeting of hcSOM reflects microbial communities shifting toward bacterial-like assemblages with higher enzyme efficiency (Figure 6b). This microbial adjustment reduced the stimulation of

plant productivity (particularly in woodC and rootC, Figure S6 in Supporting Information S1), in SCAMPS_DAMM relative to SCAMPS, consistent with the model's tighter coupling of moisture and temperature control.

Introducing explicit diffusion constraints fundamentally altered system behavior: decomposition became limited by substrate transport rather than temperature alone, leading to earlier equilibrium in respiration and nutrient turnover. Summer Rt was more dampened in SCAMPS_DAMM because the explicit coupling of temperature and moisture constrained microbial activity under high summer soil moisture. In the DAMM submodel, elevated liquid water limits O_2 diffusion to microsites, restricting substrate oxidation even as temperatures rise. This diffusional limitation reduces microbial respiration during warm but saturated periods, a process implicitly represented in the Q_{10} submodel of SCAMPS. As a result, SCAMPS_DAMM produces dampened summer Rt and more conservative seasonal C fluxes under warming. These results align with empirical evidence that substrate and moisture diffusion dominate respiration at near-freezing temperatures (Davidson et al., 2012; Sihi et al., 2020) and that shifts toward bacterial dominance with higher N demand reduce plant–microbe complementarity (Klarenberg et al., 2022; McMahon et al., 2011).

Overall, the SCAMPS_DAMM framework links winter microbial processes to growing-season plant responses through nutrient competition and substrate feedbacks. By explicitly representing diffusion-limited microbial respiration, the model captures a mechanistic sequence in which enhanced winter microbial N demand limits plant nutrient access, reducing summer productivity and substrate inputs. This mechanism provides a process-based explanation for the more conservative plant and respiration responses simulated by SCAMPS_DAMM and aligns with empirical evidence of coupling between microbial and plant nutrient cycling in Arctic tundra ecosystems (Koranda et al., 2023).

3.4. Sensitivity of Winter-Warming Responses to Model Parameters

Model sensitivity was evaluated by varying plant and microbial nutrient uptake rates (±10%) and temperature-sensitivity parameters (Q_{10} for SCAMPS; E_a, and α for SCAMPS_DAMM) within empirically constrained ranges based on Eight Mile Lake soil temperature data (Figure 3a, Table S4 in Supporting Information S1). Across 50 iterations, SCAMPS exhibited lower sensitivity in belowground (2%) and plant C (6%) pools at YR 100 (Figures S8a and S8b in Supporting Information S1) than SCAMPS_DAMM (10% belowground C, 18% plant C), with the latter's variability driven largely by its temperature-dependent diffusion submodel (Figures S8c and S8d in Supporting Information S1).

The greater responsiveness of SCAMPS_DAMM reflects its capacity to capture coupled temperature–moisture interactions. In contrast, the narrower parameter range in SCAMPS may indicate reduced flexibility rather than higher predictive accuracy, as the simpler Q_{10} formulation cannot adjust to shifts in substrate or water availability under warming. These results reinforce that model framework, in this case, explicit versus implicit diffusional control representation drives divergence in projected C–N trajectories.

4. Conclusions and Future Direction

This study shows that explicitly representing temperature-dependent diffusion constraints substantially alter projections of soil C and N cycling under winter warming in high-latitude ecosystems. Incorporating freeze–thaw dynamics with abiotic–biotic interactions changed simulated ecosystem C and N pool trajectories in line with recent empirical studies from tundra warming experiments (refs), indicating that such processes should be represented explicitly to capture tundra responses to climate change. The SCAMPS_DAMM framework predicted lower belowground C losses, shifts in decomposer-targeted SOC pools, and modest redistribution of C and N from below-to aboveground components, illustrating the influence of physical diffusion limits on C feedbacks.

While SCAMPS_DAMM increases model sensitivity and complexity, its explicit representation of diffusion constraints reveals process-level differences that could substantially alter future carbon projections in permafrost soils. Thus, incorporating similar formulations into large-scale models is warranted where data permit. Improved field measurements of soil liquid water, ice content, and seasonal C fluxes are critical for constraining mechanistic parameters. When such data are available, we recommend adopting frameworks like SCAMPS_DAMM that explicitly represent temperature- and moisture-driven diffusion processes to enhance process-based understanding of permafrost ecosystem responses to climate change. Our findings highlight that explicitly representing

diffusion and freeze–thaw constraints could reduce biases in Earth system model projections of winter C fluxes and improve representation of shoulder-season processes.

Disclaimer

None.

Conflict of Interest

The authors declare no conflicts of interest relevant to this study.

Data Availability Statement

Code and data for this study are included in Supporting Information S1 SCAMPS modeling code.zip and at https://doi.org/10.5281/zenodo.17517570 Sistla and Savage (2025). Flux observations and soil temperature and moisture data from Eight Mile Lake (EML), used to parameterize the DAMM model, are available at https://daac.ornl.gov/cgi-bin/dsviewer.pl?ds_id=1869 (Minions et al., 2024) and https://daac.ornl.gov/cgi-bin/dsviewer.pl?ds_id=1762 (Minions et al., 2020).

Acknowledgments
We would like to thank Grace Pold for initiating the code transfer to make SCAMPS broadly accessible and providing guidance on model integration. *Financial Support*: NSF-1911532 and NSF-2034304 to S.M.Natali; NSF-2034323 to S.Sistla.

References

Arndt, K. A., Hashemi, J., Natali, S. M., Schiferl, L. D., & Virkkala, A. M. (2023). Recent advances and challenges in monitoring and modeling non-growing season carbon dioxide fluxes from the Arctic Boreal Zone. *Current Climate Change Reports*, *9*(2), 27–40. https://doi.org/10.1007/s40641-023-00190-4

Arndt, K. A., Oechel, W. C., Goodrich, J. P., Bailey, B. A., Kalhori, A., Hashemi, J., et al. (2019). Sensitivity of methane emissions to later soil freezing in Arctic tundra ecosystems. *Journal of Geophysical Research: Biogeosciences*, *124*(8), 2595–2609. https://doi.org/10.1029/2019JG005242

Bond-Lamberty, B., & Thomson, A. (2010). Temperature-associated increases in the global soil respiration record. *Nature*, *464*(7288), 579–582. https://doi.org/10.1038/nature08930

Bracho, R., Natali, S., Pegoraro, E., Crummer, K. G., Schädel, C., Celis, G., et al. (2016). Temperature sensitivity of organic matter decomposition of permafrost-region soils during laboratory incubations. *Soil Biology and Biochemistry*, *97*, 1–14. https://doi.org/10.1016/j.soilbio.2016.02.008

Bruhwiler, L., Parmentier, F. J. W., Crill, P., Leonard, M., & Palmer, P. I. (2021). The Arctic carbon cycle and its response to changing climate. *Current Climate Change Reports*, *7*(1), 14–34. https://doi.org/10.1007/s40641-020-00169-5

Buckeridge, K. M., Banerjee, S., Siciliano, S. D., & Paul, G. (2013). The seasonal pattern of soil microbial community structure in mesic low Arctic tundra. *Soil Biology and Biochemistry*, *65*, 338–347. https://doi.org/10.1016/j.soilbio.2013.06.012

Byrne, B., Liu, J., Yi, Y., Chatterjee, A., Basu, S., Cheng, R., et al. (2022). Multi-year observations reveal a larger than expected autumn respiration signal across northeast Eurasia. *Biogeosciences*, *19*, 4779–4799. https://doi.org/10.5194/bg-19-4779-2022

Commane, R., Lindaas, J., Benmergui, J., Luus, K. A., Chang, R. Y. W., Daube, B. C., et al. (2017). Carbon dioxide sources from Alaska driven by increasing early winter respiration from Arctic tundra. *Proceedings of the National Academy of Sciences*, *114*(21), 5361–5366. https://doi.org/10.1073/pnas.1618567114

Davidson, E. A., Janssen, I. A., & Luo, Y. (2006). On the variability of respiration in terrestrial ecosystems: Moving beyond Q_{10}. *Global Change Biology*, *12*(2), 154–164. https://doi.org/10.1111/j.1365-2486.2005.01065.x

Davidson, E. A., Samanta, S., Caramori, S. S., & Savage, K. (2012). The Dual Arrhenius and Michaelis-Menten kinetics model for decomposition of soil organic matter at hourly to seasonal time scales. *Global Change Biology*, *18*, 1–384. https://doi.org/10.1111/j.1365-2486.2011.02546.x

Grogan, P. (2012). Cold season respiration across a low Arctic Landscape: The influence of vegetation type, snow depth, and interannual climatic variation. *Arctic Antarctic and Alpine Research*, *44*(4), 446–456. https://doi.org/10.1657/1938-4246-44.4.446

He, Y., Yang, J., Zhuang, Q., McGuire, A. D., Zhu, Q., Liu, Y., & Teskey, R. O. (2014). Uncertainty in the fate of soil organic carbon: A comparison of three conceptually different soil decomposition models. *Journal of Geophysical Research: Biogeosciences*, *119*(9), 1892–1905. https://doi.org/10.1002/2014JG002701

Hicks Pries, C. E., Schuur, E. A. G., Natali, S. M., & Crummer, K. G. (2016). Old soil carbon losses increase with ecosystem respiration in experimentally thawed tundra. *Nature Climate Change*, *6*(2), 214–218. https://doi.org/10.1038/nclimate2830

Huang, J., Zhang, X., Zhang, Q., Lin, Y., Hao, M., Luo, Y., et al. (2017). Recently amplified Arctic warming has contributed to a continual global warming trend. *Nature Climate Change*, *7*(12), 875–879. https://doi.org/10.1038/s41558-017-0009-5

Hugelius, G., Ramage, J., Burke, E., Chatterjee, A., Smallman, T. L., Aalto, T., et al. (2024). Permafrost region greenhouse gas budgets suggest a weak CO_2 sink and CH_4 and N_2O sources, but magnitudes differ between top-down and bottom-up methods. *Global Biogeochemical Cycles*, *38*(10), e2023GB007969. https://doi.org/10.1029/2023GB007969

Hugelius, G., Strauss, J., Zubrzycki, S., Harden, J. W., Schuur, E. A. G., Ping, C.-L., et al. (2014). Estimated stocks of circumpolar permafrost carbon with quantified uncertainty ranges and identified data gaps. *Biogeosciences*, *11*(23), 6573–6593. https://doi.org/10.5194/bg-11-6573-2014

IPCC. (2019). In P. R. Shukla, J. Skea, E. Calvo Buendia, V. Masson-Delmotte, H.-O. Pörtner, et al. (Eds.), *Climate Change and Land: An IPCC special report on climate change, desertification, land degradation, sustainable land management, food security, and greenhouse gas fluxes in terrestrial ecosystems*.

Kirschbaum Miko, U. F. (1995). The temperature dependence of soil organic matter decomposition, and the effect of global warming on soil organic C storage. *Soil Biology and Biochemistry*, *27*(6), 753–760. https://doi.org/10.1016/0038-0717(94)00242-S

Klarenberg, I. J., Keuschnig, C., Russi Colmenares, A. J., Warshan, D., Jungblut, A. D., Jónsdóttir, I. S., & Vilhelmsson, O. (2022). Long-term warming effects on the microbiome and nifH gene abundance of a common moss species in sub-Arctic tundra. *New Phytologist*, *234*(6), 2044–2056. https://doi.org/10.1111/nph.17837

Koenigk, T., Brodeau, L., Graversen, R. G., Karlsson, J., Svensson, G., Tjernström, M., et al. (2013). Arctic climate change in 21st century CMIP5 simulations with EC-Earth. *Climate Dynamics*, *40*(11), 2719–2743. https://doi.org/10.1007/s00382-012-1505-y

Koranda, M., Rinnan, R., & Michelsen, A. (2023). Close coupling of plant functional types with soil microbial community composition drives soil carbon and nutrient cycling in tundra heath. *Plant and Soil*, *488*(1–2), 551–572. https://doi.org/10.1007/s11104-023-05993-w

Kurylyk, B. L., & Watanabe, K. (2013). The mathematical representation of freezing and thawing processes in variably-saturated, nondeformable soils. *Advances in Water Resources*, *60*, 160–177. https://doi.org/10.1016/j.advwatres.2013.07.016

Liu, Y., Riley, W. J., Keenan, T. F., Mekonnen, Z. A., Holm, J. A., Zhu, Q., & Torn, M. S. (2022). Dispersal and fire limit Arctic shrub expansion. *Nature Communications*, *13*(1), 3843. https://doi.org/10.1038/s41467-022-31597-6

Liu, Z., Rogers, B. M., Keppel-Aleks, G., Helbig, M., Ballantyne, A. P., Kimball, J. S., et al. (2024). Seasonal CO_2 amplitude in northern high latitudes. *Nature Reviews Earth & Environment*, *5*(11), 802–881. https://doi.org/10.1038/s43017-024-00600-7

Mauritz, M., Schuur, E. A., & LTER, B. C. (2016). *Eight mile lake research watershed, carbon in permafrost experimental heating research (CiPEHR): Weekly dark CO_2 fluxes, 2014 ver 3*. Environmental Data Initiative. https://doi.org/10.6073/pasta/03be8430f5cea48ffe856ca3e8947d1d

McMahon, S. K., Wallenstein, M. D., & Schimel, J. P. (2011). A cross-seasonal comparison of active and total bacterial community composition in Arctic tundra soil using bromodeoxyuridine labeling. *Soil Biology and Biochemistry*, *43*(2), 287–295. https://doi.org/10.1016/j.soilbio.2010.10.013

Mikan, C. J., Schimel, J. P., & Doyle, A. P. (2002). Temperature controls of microbial respiration in Arctic tundra soils above and below freezing. *Soil Biology and Biochemistry*, *34*(11), 1785–1795. https://doi.org/10.1016/S0038-0717(02)00168-2

Minions, C., Natali, S., Watts, J. D., & Ludwig, S. (2024). ABoVE: Soil temperature and VWC at unburned and burned sites across Alaska, 2016-2023 [Dataset]. *ORNL DAAC, Oak Ridge, Tennessee, USA*. https://doi.org/10.3334/ORNLDAAC/1869

Minions, C., Natali, S., Watts, J. D., Ludwig, S., & Risk, D. (2020). ABoVE: Year-round soil CO_2 efflux in Alaskan Ecosystems, Version 2.1 [Dataset]. *ORNL Distributed Active Archive Center*. https://doi.org/10.3334/ORNLDAAC/1762

Myers-Smith, I. H., Kerby, J. T., Phoenix, G. K., Bjerke, J. W., Epstein, H. E., Assmann, J. J., et al. (2020). Complexity revealed in the greening of the Arctic. *Nature Climate Change*, *10*(2), 106–117. https://doi.org/10.1038/s41558-019-0688-1

Natali, S. M., Schuur, E. A. G., & Rubin, R. L. (2012). Increased plant productivity in Alaskan tundra as a result of experimental warming of soil and permafrost. *Journal of Ecology*, *100*(2), 488–498. https://doi.org/10.1111/j.1365-2745.2011.01925.x

Natali, S. M., Schuur, E. A. G., Webb, E. E., Pries, C. E. H., & Crummer, K. G. (2014). Permafrost degradation stimulates carbon loss from experimentally warmed tundra. *Ecology*, *95*(3), 602–608. https://doi.org/10.1890/13-0602.1

Natali, S. M., Watts, J. D., Rogers, B. M., Potter, S., Ludwig, S. M., Selbmann, A. K., et al. (2019). Large loss of CO_2 in winter observed across the northern permafrost region. *Nature Climate Change*, *9*(11), 852–857. https://doi.org/10.1038/s41558-019-0592-8

Outcalt, S. I., Nelson, F. E., & Hinkel, K. M. (1990). The zero-curtain effect: Heat and mass transfer across an isothermal region in freezing soil. *Water Resources Research*, *26*(7), 1509–1516. https://doi.org/10.1029/WR026i007p01509

Panikov, N. S., & Sizova, M. V. (2007). Growth kinetics of microorganisms isolated from Alaskan soil and permafrost in solid media frozen down to -35°C. *FEMS Microbiology Ecology*, *59*(2), 500–512. https://doi.org/10.1111/j.1574-6941.2006.00210.x

Pedron, S. A., Welker, J. M., Euskirchen, E. S., Klein, E. S., Walker, J. C., Xu, X., & Czimczik, C. I. (2022). Closing the winter gap—Year-round measurements of soil CO_2 emission sources in Arctic tundra. *Geophysical Research Letters*, *49*(6), e2021GL097347. https://doi.org/10.1029/2021GL097347

Pold, G., Kwiatkowski, B., Rastetter, E., & Sistla, S. (2022). Sporadic P limitation constrains microbial growth and facilitates SOM accumulation in the stoichiometrically coupled, acclimating microbe–plant–soil model. *Soil Biology and Biochemistry*, *165*, 108489. https://doi.org/10.1016/j.soilbio.2021.108489

Poppeliers, S. W. M., Hefting, M., Dorrepaal, E., & Weedon, J. T. (2022). Functional microbial ecology in arctic soils: The need for a year-round perspective. *FEMS Microbial Ecology*, *98*(12), fiac134. PMID: 36368693; PMCID: PMC9701097. https://doi.org/10.1093/femsec/fiac134

Rantanen, M., Karpechko, A. Y., Lipponen, A., Nordling, K., Hyvärinen, O., Ruosteenoja, K., et al. (2022). The Arctic has warmed nearly four times faster than the globe since 1979. *Communications Earth & Environment*, *3*(1), 168. https://doi.org/10.1038/s43247-022-00498-3

Rastetter, E. B., Agren, G. I., & Shaver, G. R. (1997). Response of N-limited ecosystems to increased CO_2: A balanced-nutrition, coupled-element-cycles model. *Ecological Applications*, *7*(2), 444–460. https://doi.org/10.2307/2269511

Rastetter, E. B., Yanai, R. D., Thomas, R. Q., Vadeboncoeur, M. A., Fahey, T. J., Fisk, M. C., et al. (2013). Recovery from disturbance requires resynchronization of ecosystem nutrient cycles. *Ecological Applications*, *23*(3), 621–642. https://doi.org/10.1890/12-0751.1

R Core Team. (2021). *R: A language and environment for statistical ## computing*. R Foundation for Statistical Computing. Retrieved from https://www.R-Project.Org/

Romanovsky, V. E., & Osterkamp, T. E. (2000). Effects of unfrozen water on heat and mass transport processes in the active layer and permafrost. *Permafrost Periglac*, *11*(3), 219–239. https://doi.org/10.1002/1099-1530(200007/09)11:3<219::aid-ppp352>3.0.co;2-7

Schaefer, K., & Jafarov, E. (2016). A parameterization of respiration in frozen soils based on substrate availability. *Biogeosciences*, *13*(7), 1991–2001. https://doi.org/10.5194/bg-13-1991-2016

Schuur, E. A. G., Vogel, J., Crummer, K., Lee, H., Sickman, J. O., & Osterkamp, T. E. (2009). The effect of permafrost thaw on old carbon release and net carbon exchange from tundra. *Nature*, *459*(7246), 556–559. https://doi.org/10.1038/nature08031

Schuur, E. A. G., Crummer, K. G., Vogel, J. G., & Mack, M. C. (2007). Plant species composition and productivity following permafrost thaw and thermokarst in Alaskan Tundra. *Ecosystems*, *10*(2), 280–292. https://doi.org/10.1007/s10021-007-9024-0

Sihi, D., Davidson, E. A., Savage, K. E., & Liang, D. (2020). Simultaneous numerical representation of soil microsite production and consumption of carbon dioxide, methane, and nitrous oxide using probability distribution functions. *Global Change Biology*, *26*, 1–218. https://doi.org/10.1111/gcb.14855

Sinsabaugh, R. L., Carreiro, M. M., & Repert, D. A. (2002). Allocation of extracellular enzymatic activity in relation to litter composition, N deposition, and mass loss. *Biogeochemistry*, *60*, 1–24. https://doi.org/10.1023/a:1016541114786

Sinsabaugh, R. L., Lauber, C. L., Weintraub, M. N., Ahmed, B., Allison, S. D., Crenshaw, C., et al. (2008). Stoichiometry of soil enzyme activity at global scale. *Ecology Letters*, *11*, 1252–1264. https://doi.org/10.1111/j.1461-0248.2008.01245.x

Sistla, S., Moore, J., Simpson, R., Laura, G., Shaver, G., & Schimel, J. (2013). Long-term warming restructures Arctic tundra without changing net soil carbon storage. *Nature*, *497*(7451), 615–618. https://doi.org/10.1038/nature12129

Sistla, S., & Savage, K. (2025). Inclusion of explicit soil freeze-thaw dynamics in an arctic ecosystem model constrains winter warming driven carbon loss [Software]. *Zenodo*. https://doi.org/10.5281/zenodo.17517570

Sistla, S. A., Rastetter, E. B., & Schimel, J. P. (2014). Responses of a tundra system to warming using SCAMPS: A stoichiometrically coupled, acclimating microbe—Plant—Soil model. *Ecological Monographs*, *84*(1), 151–170. https://doi.org/10.1890/12-2119.1

Soetaert, K., & Petzoldt, T. (2010). Inverse modelling, sensitivity and Monte Carlo analysis in R using package FME. *Journal of Statistical Software*, *33*(3), 1–28. https://doi.org/10.18637/jss.v033.i03

Soetaert, K., Petzoldt, T., & Setzer, R. W. (2010). Solving differential equations in *R*: Package deSolve. *Journal of Statistical Software*, *33*, 9. https://doi.org/10.18637/jss.v033.i09

Sommerfeld, R. A., Mosier, A. R., & Musselman, R. C. (1993). CO_2, CH_4 and N_2O flux through a Wyoming snowpack and implications for global budgets. *Nature*, *361*(6408), 140–142. https://doi.org/10.1038/361140a0

Stackhouse, B. T., Vishnivetskaya, T. A., Layton, A., Chauhan, A., Pfiffner, S., Mykytczuk, N. C., et al. (2015). Effects of simulated spring thaw of permafrost from mineral cryosol on CO_2 emissions and atmospheric CH_4 uptake. *Journal of Geophysical Research: Biogeosciences*, *120*(9), 1764–1784. https://doi.org/10.1002/2015JG003004

Sturm, M., Schimel, J., Michaelson, G., Welker, J. M., Oberbauer, S. F., Liston, G. E., et al. (2005). Winter biological processes could help convert arctic tundra to shrubland. *BioScience*, *55*(1), 17–26. https://doi.org/10.1641/0006-3568(2005)055[0017:wbpchc]2.0.co;2

Talamucci, F. (2003). Freezing processes in porous media: Formation of ice lenses, swelling of the soil. *Mathematical and Computer Modelling*, *37*(5–6), 595–602. https://doi.org/10.1016/S0895-7177(03)00053-0

Tao, J., Zhu, Q., Riley, W. J., & Neumann, R. B. (2021). Improved ELMv1-ECA simulations of zero-curtain periods and cold-season CH_4 and CO_2 emissions at Alaskan Arctic tundra sites. *The Cryosphere*, *15*(12), 5281–5307. https://doi.org/10.5194/tc-15-5281-2021

Tarnocai, C., Canadell, J., Schuur, E., Kuhry, P., Mazhitova, G., & Zimov, S. (2009). Soil organic carbon pools in the northern circumpolar permafrost region. *Global Biogeochemical Cycles*, *23*(2). https://doi.org/10.1029/2008gb003327

Tilston, E. L., Sparrman, T., & Öquist, M. G. (2010). Unfrozen water content moderates temperature dependence of sub-zero microbial respiration. *Soil Biology and Biochemistry*, *42*(9), 1396–1407. https://doi.org/10.1016/j.soilbio.2010.04.018

Trivedi, P., Batista, B. D., Bazany, K. E., & Singh, B. K. (2022). Plant–microbiome interactions under a changing world: Responses, consequences and perspectives. *New Phytologist*, *234*(6), 1951–1959. https://doi.org/10.1111/nph.18016

van Vuuren, D. P., Edmonds, J., Kainuma, M., Riahi, K., Thomson, A., Hibbard, K., et al. (2011). The representative concentration pathways: An overview. *Climatic Change*, *109*(1–2), 5–31. https://doi.org/10.1007/s10584-011-0148-z

Walsh, J. E., Bhatt, U. S., Littell, J. S., Leonawicz, M., Lindgren, M., Kurkowski, T. A., et al. (2018). Downscaling of climate model output for Alaskan stakeholders. *Environmental Modelling & Software*, *110*, 38–51. https://doi.org/10.1016/j.envsoft.2018.03.021

Wang, T., Ciais, P., Piao, S. L., Ottlé, C., Brender, P., Maignan, F., et al. (2011). Controls on winter ecosystem respiration in temperate and boreal ecosystems. *Biogeosciences*, *8*(7), 2009–2025. https://doi.org/10.5194/bg-8-2009-2011

Watts, J. D., Potter, S., Rogers, B. M., Virkkala, A. M., Fiske, G., Arndt, K. A., et al. (2024). Regional hotspots of change in northern high latitudes informed by observation from space. *Geophysical Research Letters*, *52*, e2023GL108081. https://doi.org/10.5194/bg-8-2009-2011

Webb, E. E., Schuur, E. A. G., Natali, S. M., Oken, K. L., Bracho, R., Krapek, J. P., et al. (2016). Increased wintertime CO_2 loss as a result of sustained tundra warming. *Journal of Geophysical Research: Biogeosciences*, *121*(2), 249–265. https://doi.org/10.1002/2014JG002795

Zhou, L., Sommers, P., Schmidt, S. K., Magnani, M., Cimpoiasu, M., Oliver, K., et al. (2024). Seasonal dynamics of Arctic soils: Capturing year-round processes in measurements and soil biogeochemical models. *Earth-Science Reviews*, *254*, 104820. https://doi.org/10.1016/j.earscirev.2024.104820